Seismic Anisotropy beneath Northern Victoria Land from SKS Splitting Analysis

Silvia Pondrelli[1] · **Lucia Margheriti**[2] · **Stefania Danesi**[2]
[1] Istituto Nazionale di Geofisica e Vulcanologia, Via D. Creti 12, 40128 Bologna, Italy, <pondrelli@bo.ingv.it>
[2] Istituto Nazionale di Geofisica e Vulcanologia, Via di Vigna Murata 605, 00143 Rome, Italy

Abstract. Teleseismic data recorded by temporary and permanent stations located in the Northern Victoria Land region are analysed in order to identify the presence and location of seismic anisotropy. We work on data recorded by 24 temporary seismographic stations deployed between 1993 and 2000 in different zones of the Northern Victoria Land, and by the permanent very broad-band stations TNV located near the Italian Base "M. Zucchelli". The temporary networks monitored an area extending from Terra Nova Bay towards the South beyond the David Glacier and up to the Indian Ocean northward. To better constrain our study, we also provide an analysis of data recorded by TNV in the same period of time and we take into account also SKS shear wave splitting measurements performed by Barruol and Hoffman (1999) on data recorded by DRV. This study, to be considered as preliminary, reveals the presence of seismic anisotropy below the study region, with a mainly NW-SE fast velocity direction below the Terra Nova Bay area and rather large delay times, that mean a deep rooted anisotropic layer.

Introduction

The study region, the northern Victoria Land, is mainly characterized by the presence of the Transantarctic Mountains, that border the Ross Sea all along this region. From the tectonic point of view, this high-elevated belt, extending for more than 2 500 km, is considered an asymmetric rift shoulder segmented by several transverse fault systems (Fig. 3.8-1; Behrent et al. 1991; Salvini et al. 1997; Wilson 1999). The origin of the West Antarctic Rift, mainly constitued by the Ross Embayment, is still object of debate. The first hypothesis was to relate it to an active plume centered below Marie Byrd Land (Behrendt et al. 1991), but recently some investigations revealed a complex Cenozoic geodynamic, mainly due to the activation of intraplate right-lateral strike-slip structures, inducing a strong oblique component in the rifting process. The examination of these major tectonic structures may support a transtension-related source for the extension which designed the Ross Sea Embayment and the volcanism related to it (Salvini et al. 1997; Rocchi et al. 2002).

The transition from the Ross Sea extensional basin to the Transantarctic Mountains is abrupt, with a Moho detected at less than 20 km of depth in the Ross Sea and increasing up to more than 40 km of depth beneath the mountain chain (Di Bona et al. 1997 and references therein; Pondrelli et al. 1997; Bannister et al. 2003). This sharp variation marks the presence of a strongly heterogeneous crustal and lithospheric structure. Surface wave tomography as well clearly indicates that the northern Victoria Land region is on the boundary of the East Antarctica craton and the West Antarctic Rift System (Ritzwoller et al. 2003; Danesi and Morelli 2001). A dra-

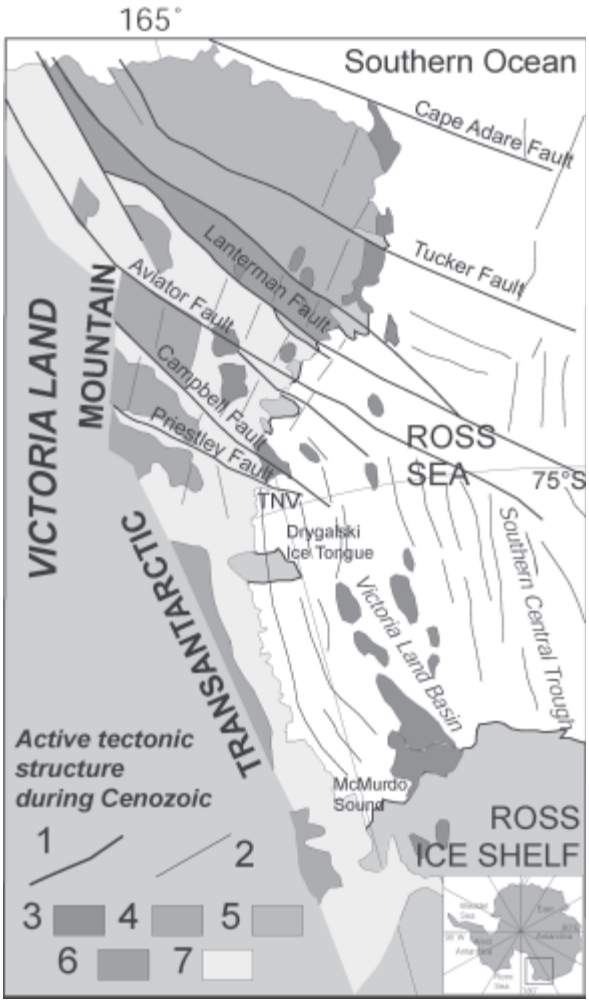

Fig. 3.8-1. Tectonic sketch map of Victoria Land (modified from Salvini et al. 1997). Legend 1, 2, 3 …???

From: Fütterer DK, Damaske D, Kleinschmidt G, Miller H, Tessensohn F (eds) (2005) Antarctica: Contributions to global earth sciences. Springer-Verlag, Berlin Heidelberg New York, pp 153–160

matic discontinuity in shear wave velocity pattern (see Fig. 4 in Morelli and Danesi, 2004) marks the limit between the Archean shield and the Ross Sea lithosphere, the former showing deep cold continental roots down to 250–300 km (Morelli and Danesi 2004), the latter anomalously warm and stretched. The depth to which seismic tomography can reliably image the Antarctic region is however hampered to 350–400 km, which is not enough to undoubtedly confirm or disprove the presence of a mantle plume head beneath West Antarctica.

Shear wave splitting is generally considered as caused by lattice preferred orientation of anisotropic minerals of the mantle, as olivine (Vinnik et al. 1989; Silver 1996; Savage 1999). Measurements from teleseismic SKS phases are a powerfull instrument to constrain the strain pattern in the mantle, extending the geological analysis at depth and helping in the interpretation of lithosphere kinematics. When shear-waves travel in an anisotropic material, they split into two polarized waves travelling at different velocities. Polarization direction ϕ and time delay δt between these two phases characterise the anisotropy. To detect the presence of seismic anisotropy beneath Northern Victoria Land and to study its relation with the geodynamic of this region, we analyze seismographic data recorded during temporary deployments and by TNV; moreover, we take into account the results of SKS measurements obtained by Barruol and Hoffman (1999) from DRV data records.

Sations and Dataset

Since 1993 several temporary geophysical campaigns have been performed in the Terra Nova Bay region (Cimini et al. 1995; Pondrelli et al. 1997; Della Vedova et al. 1997). On the total we have data to analyze from 24 temporary stations (Table 3.8-1). Most of them were located in the area

Table 3.8-1.
Station coordinates and recording times

Station name	Latitude	Longitude	Recording time
ALF9	–75.898	162.58	Dec 1993–Jan 1994
BRA9	–75.83	160.5	Dec 1993–Jan 1994
BT01	–71.11	166.563	Dec 1999
BT02	–71.206	164.512	Dec 1999
BT03	–71.417	162.060	Dec 1999–Jan 2000
BT04	–70.736	159.991	Dec 1999–Jan 2000
BT05	–69.890	158.928	Dec 1999–Jan 2000
BT06	–69.51	157.34	Jan 2000
BT65	–69.354	156.129	Jan 2000
BT07	–69.25	155	Jan 2000
BT08	–68.98	154.19	Jan 2000
CHA9	–75.75	158.3	Dec 1993–Jan 1994
CPW9	–74.63	165.43	1993–1994; 1994–1995; 1997–1998
DEL9	–75.697	157.08	Dec 1993–Jan 1994
ESK9	–74.3	162.65	1995–1996; 1997–1998
INX9	–74.934	163.708	1997–1998
KNT9	–74.53	163.97	1995–1996
MDK9	–74.4	163.97	1993–1994; 1994–1995; 1997–1998
MEL9	–74.32	165.02	1993–1994; 1994–1995; 1997–1998
NAN9	–74.579	162.615	1995–1996; 1997–1998
OAS9	–74.69	164.1	1993–1994; 1994–1995; 1995–1996
OSC9	–74.56	164.85	1997–1998
SKR9	–74.58	161.94	1995–1996; 1997–1998
TNF9	–74.993	162.744	1995–1996; 1997–1998
TNV	–74.7	164.12	Permanent

Table 3.8-2. Station name, event date and location, delta and backazimuth, and fast direction measurements with errors

Station	Event				Ev.-St. distance	Backaz	Fast direct. φ	dφ	Delay time	dt
	Date (yy/mm/dd)	Latitude	Longitude	Depth						
ALF9	94/01/10	–13.33	–69.44	596	85.7	129.7	129.7		null	
BRA9	94/01/10	–13.33	–69.44	596	86.1	131.7	51	2	0.9	0.13
BT06	00/01/21	13.15	125.75	33	85.4	329.2	27	14	0.96	2.05
BT07	00/01/28	26.08	124.5	193	97.6	332.6	332.6		null	
BT08	00/01/28	26.08	124.5	193	97.2	333.3	–7	5	2.16	0.15
CPW9	93/11/29	10.29	126.47	38	88.1	321.8	68	2	2.04	0.26
	97/11/28	–13.74	–68.79	586	85.6	127.8	51	2	1.75	0.22
	98/01/01	23.91	141.91	95	99.5	338.3	23	8	0.55	0.07
ESK9	95/12/03	44.66	149.3	33	119.0	349.1	11	12	1.65	0.57
	97/11/21	22.21	92.7	54	106.0	295.1	59	5	1.7	0.15
	97/12/11	3.93	–75.79	177	102	119.7	–89	9	1.25	0.3
	97/12/18	14.71	144.65	33	89.6	342.6	–78	2	1.35	0.1
	98/01/01	23.91	141.91	95	98.9	340.9	34	4	1.5	0.18
	98/01/10	14.37	–91.47	33	108.0	101.4	–88	6	1.75	0.75
KNT9	95/12/03	44.66	149.3	33	119.3	348.0	33	10	0.7	0.12
MDK9	97/12/18	14.71	144.65	33	89.8	341.3	33	8	0.6	1.22
	98/01/14	–2.11	68.09	10	89.6	263.8	46	6	0.8	0.12
	98/02/11	10.33	124.99	56	88.0	321.7	16	4	2.35	0.23
MEL9	93/12/10	20.91	121.28	12	99.1	319.9	30	6	2.18	0.18
	97/11/28	–13.74	–68.79	586	85.9	128.2	128.2		null	
	98/01/01	23.91	141.91	95	99.2	340.9	58	2	1.9	2.98
	98/01/10	14.37	–91.47	33	107.4	99.1	–53	6	1.4	0.28
NAN9	97/11/15	43.81	145.02	161	118.7	345.6	25	4	1.05	0.12
OAS9	93/11/29	10.29	126.47	38	87.9	323.0	47	18	0.8	0.2
OSC9	97/11/28	–13.74	–68.79	586	85.8	128.3	128.3		null	
	97/12/11	3.93	–75.79	177	101.3	117.5	61	12	0.85	0.23
	97/12/18	14.71	144.65	33	90.0	340.5	54	3	1.95	0.25
	98/01/01	23.91	141.91	95	99.3	338.8	56	2	2.8	0.38
	98/01/10	14.37	–91.47	33	107.4	99.3	31	9	0.8	1.58
SKR9	97/12/11	3.93	–75.79	177	102.0	120.4	42	2	1.7	0.3
TNF9	98/02/03	15.88	–96.3	33	108.1	96.4	96.4		null	
TNV	91/04/22	9.68	–83.08	10	105.2	109.0	42	8	2.25	0.45
	92/01/20	27.96	139.33	512	103.5	337.1	337.1		null	
	93/01/15	43.4	143.26	100	118.4	342.4	–1	12	2.15	0.67
	93/01/19	38.63	133.46	455	114.7	333.4	15	16	1.1	2.23
	95/01/16	34.55	135	16	110.5	334.1	334.1		null	
	95/01/19-1	5.07	–72.92	18	103.2	120.2	47	7	3	0.65
	95/01/19-2	43.33	146.72	63	118.1	345.4	56	6	1.65	0.3
	96/11/21	6.66	126.46	53	85.3	321.8	–69	4	2.15	0.23
	97/11/15	43.81	145.02	161	118.7	343.9	20	16	0.85	0.23
	97/11/21	22.21	92.7	54.4	106.5	293.2	54	14	1.3	0.38
	97/11/28	–13.74	–68.79	586	85.9	128.5	56	6	1.65	0.63
	98/04/03	–8.15	–74.24	164.6	90.1	122.0	67	12	1.55	1.27
	98/05/03	22.31	125.31	33	99.8	323.4	323.4		null	
	98/06/07	15.96	–93.78	86.6	108.4	96.7	45	22	1.6	2.78
	98/06/18	–11.57	–13.89	10	94.2	181.4	65	12	1.55	1.27
	98/08/04	–0.59	–80.39	33	96.0	114.2	42	6	3	0.57
	98/08/23	11.66	–88.04	54.6	105.8	103.6	49	14	2.75	0.88
	98/09/22	11.82	143.15	9.2	87.1	338.9	338.9		null	
	98/10/03	28.5	127.61	226.6	105.5	326.6	326.6		null	

around the Italian M. Zucchelli Station and had multiple reoccupations (up to five campaigns, from 1993 to 2000), recording the larger amount of data. On the contrary, northernmost and southernmost sites, respectively related to the last campaign, in 2000, and to the ACRUP1 experiment performed in 1994 (Della Vedova et al. 1997), are those for which only one occupation was done and consequently scarce data were recorded. In the region, the permanent Italian very broad-band seismographic station TNV has been recording continuously since 1989 to present and data availability is rather large.

We selected from NEIS Catalog (http://www.neic.cr.usgs.gov/neis/epic/epic.html) all earthquakes with a magnitude greater than 5.5 occurred during the recording times (from 1993 to 2000), located at a distance between 85° and 120° from our seismographic stations, to collect SKS phases of sufficient energy. The collected dataset includes more than 100 teleseisms, and more than a half of them gave good results (Table 3.8-2). However, only for TNV permanent station the azimuthal coverage was good, while for the other sites the NW and SE quadrants only were well sampled (Table 3.8-2).

Analysis and Discussion

The analysis performed here is done on teleseismic SKS phases, which travel as an S phase in the crust and mantle, as a P phase in the liquid core and convert to an S phase at the core-mantle boundary at the receiver side, polarized in the vertical plane of propagation. If SKS phases travel across an isotropic medium, all the energy propagates on the radial component only. In practice, almost all our data give splitted SKS phases, pointing out that shear waves encountered anisotropic material (Fig. 3.8-2, upper panel). The fast velocity direction ϕ, measured clockwise from the north, corresponds to the direction along which the strain aligns highly anisotropic cristals in the mantle; the delay time δt, measured between the fast and the slow components, is a quantification of the thickness of the anisotropic layer transversed by SKS phases. To determine the fast velocity direction φ and the delay time δt, we use the method of Silver and Chan (1991), that assumes that shear waves traverse a single homogeneous anisotropic layer. The method is

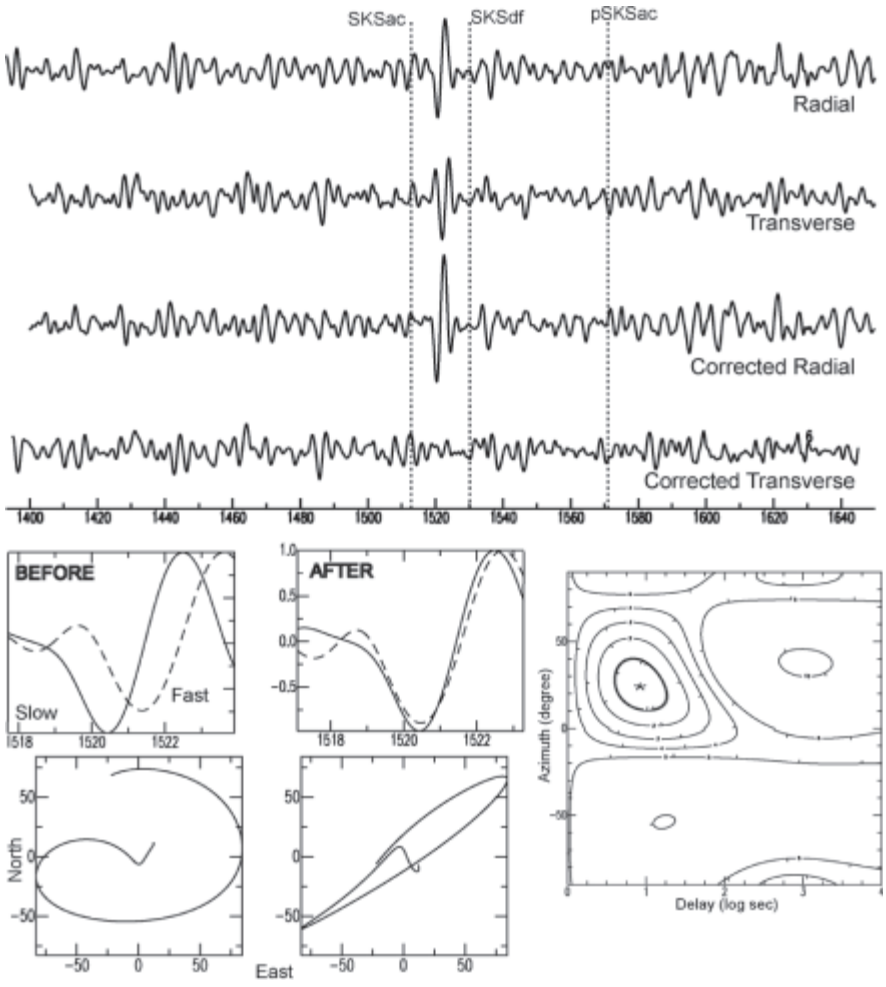

Fig. 3.8-2. Example of performed analysis; event occurred in Japan on November 15, 1997 and was recorded by NAN9 station. *Upper panel:* Radial and transverse components of seismographic recordings before and after the removal of the effect of the anisotropy. *Lower left panels:* Selected SKS phase (above) and its particle motion (below). Fast (*dotted line*) and slow (*continuous line*) phases are superimposed by the removal of the anisotropy effect. *Lower right panel:* Contour plot of the minimized energy on the corrected transverse component; the *star* is the minimum value, *first contour* is the 95% confidence region

based on a grid search over the possible splitting parameters space to find the pair of φ and δt that, when used to remove the anisotropy effect, most successfully removes its (Silver and Chan 1988). This is done by minimizing the energy on the reconstructed transverse component (upper part of Fig. 3.8-2, indicated as Corrected Radial and Transverse components). The error bounds for the estimated splitting parameters are obtained through an F-test analysis, as described by Silver and Chan (1991). When the absence of splitting is detected on the analysed waveform we have a "null" measurement, that doesn't necessarily mean that anisotropy is absent. In fact, a "null" from a single measurement also occur when the initial polarization of the shear wave is parallel to the fast or slow polarization direction of the anisotropic media. For this reason null measurements are characterized by the event back-azimuth (Table 3.8-2).

Results of our analysis reveal the presence of seismic anisotropy below the study region (Fig.3.8-3 and 3.8-4), with different directions moving from the northern to the southern part. Below DRV (Dumont D'Urville, French base) the anisotropy shows an E-W average direction (Barruol and Hoffman 1999). Going eastward, the few data available at stations BT01 to BT08 (deployed only during the 1999/2000 campaign) give a couple of N-S directions. The scarcity of data do not allow any large scale interpretation. Going southward, around the Terra Nova Bay area, our results are better constrained due to the larger amount of data recorded by multiple deployed temporary stations and by the TNV permanent station. In Fig. 3.8-4 data are mapped at the piercing point at 150 km of depth, to identify the presence of different fast velocity direction respect to different back-azimuths. It is evident that the NE-SW fast direction dominates, with also null measurements in agreement. Only few data show a different pattern, as the NW-SE trend obtained for a pair of events recorded at MEL9 or the E-W trend shown by another pair of event recorded at ESK9 (Table 3.8-2). Delay times are 1.6 s on average, and some examples show larger values with respect to world wide evaluation, indicating therefore that the anisotropy layer which splits SKS is deeply rooted. The NE-SW dominant fast velocity direction is in agreement with the Transantarctic Mountains trend, an usual observation along mountain chains, where fast direction is in general parallel to the belt axis (Savage 1999). We therefore consider that this anisotropy is related to the strain induced in the mantle by the formation of the chain; considering the deep rooted structure of the mountains belt, this hypothesis is also supported by the rather large values for the delay times. Concerning data reporting EW and NW-SE fast velocity directions, we can suggest two possible explanations: the pattern could be due to the extensional trend regime that produced the opening of the Ross Sea or, alternatively, the paths could have sampled

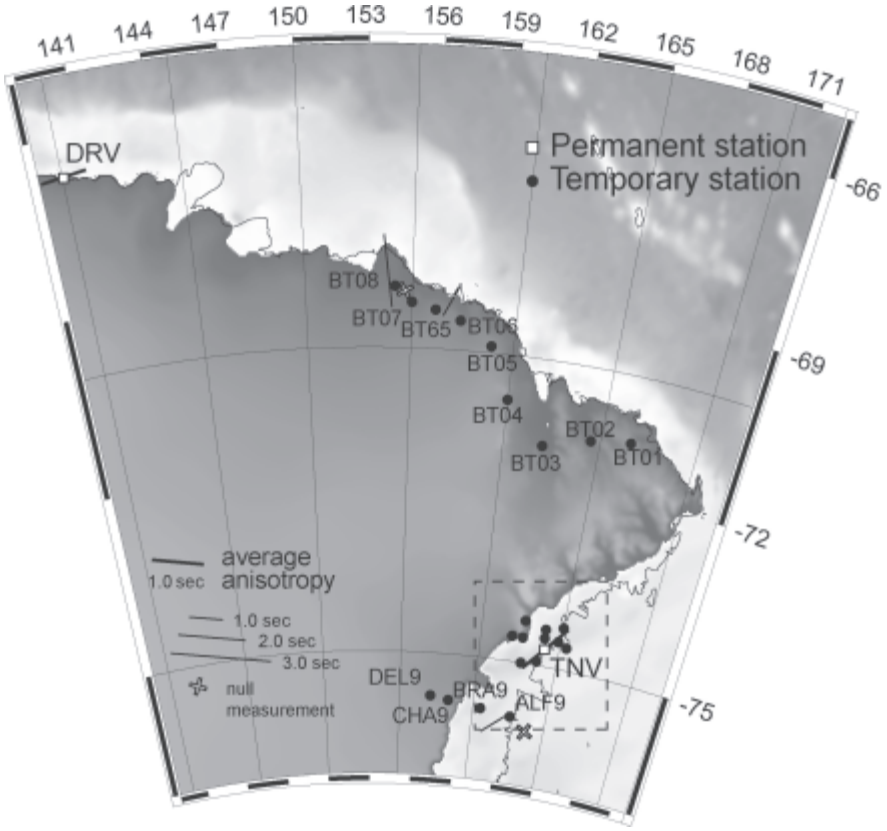

Fig. 3.8-3.
Map of all sites for which data have been analyzed. On *DRV* the average value obtained by Barruol and Hoffman (1999) is mapped. *Thick lines* are average fast direction (used here for *DRV* and *TNV*), *thin lines* are single measurements, mapped at the SKS ray piercing point at 150 km of à depth. Length of lines is proportional to the delay time. *Null measurements* are plotted with two small lines with directions parallel to the two allowed fast direction. *Inset* shows area enlarged in Fig. 3.8-4

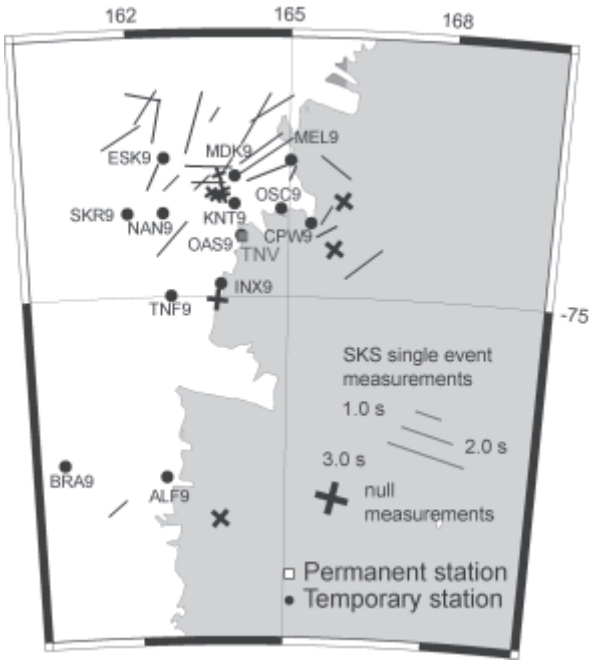

Fig. 3.8-4. Map of fast velocity direction mapped at 150 km depth piercing point for single measurements. For symbols see Fig. 3.8-3

one of the several large strike-slip NW-SE structures mapped in the northern Victoria Land (Fig. 3.8-1; Salvini et al. 1997). However, most of the out-of-trend data are related to events with a SE backazimuth, that therefore along the upward path, sample the warm and stretched lithospehere-astehosphere of the Ross Sea, while on the contrary, NE-SW fast velocity directions seems to be mainly related to data sampling the East Antarctica craton. However, the density and azimuthal distribution of obtained fast direction only allow preliminary hypotheses, that deep structure heterogeneity shown by tomographic images beneath the region (Morelli and Danesi 2004) would authorize. Certainly in the future, with a larger amount of recordings from permanent stations and from recently going on temporary deployments (e.g., Wiens et al. 2003; Bannister et al. 2003), we would better depict the characteristics of seismic anisotropy beneath Northern Victoria Land.

Conclusions

We analyzed more than 100 teleseisms recorded by 24 temporary and one, TNV, permanent stations, deployed in northern Victoria Land region. Our study produced preliminary results, that reveal the presence of seismic anisotropy beneath all of the study region, with different fast velocity direction moving from north to south. However, only around Terra Nova Bay area the data availability was large enough to better depict the anisotropy distribution. Here the dominant fast velocity direction is NE-SW, in agreement with the Transantarctic Mountains trend. Only few examples of E-W and NW-SE directions are recorded, probably due to the extensional trend that allowed the opening of Ross Sea or the presence of large strike-slip structures characterizing the Northern Victoria Land. Delay times show rather large values, on average 1.6 s, indicating that the detected anisotropic layer may be thick and deep rooted. The preliminary character of these results will be solved in the future with a hopefully larger availability of seismographic data.

Acknowledgment

We would like to thank all people involved in installation and maintenance of temporary stations and TNV permanent station. Thanks to D. Wiens and an anonymous reviewer for their useful comments.

Reference

Bannister SyuJ, Leitner B, Kennet BLN (2003) Variations in crustal structure across the transition from West to East Antarctica, Southern Victoria Land. Geophys J Internat 155:870–884

Barruol G, Hoffman R (1999) Upper mantle anisotropy beneath the Geoscope stations. J Geophys Res 104(5):10757–10773

Behrendt JC, LeMasurier WE, Cooper AK, Tessensohn F, Tréhu A, Damaske D (1991) Geophysical studies of the West Antarctic Rift System. Tectonics 10(6):1257–1273

Cimini GB, Amato A, Cerrone M, Chiappini M, Di Bona M,Pondrelli S (1995) Passive seismological studies in the Terra Nova Bay Area (Antarctica): First Results From the 1993–94 Expedition. Terra Antartica 2:81–98

Di Bona M, Amato A, Azzara R, Cimini GB, Colombo D, Pondrelli S (1997) Constraints on the lithospheric structure beneath the Terra Nova Bay area from teleseismic P to S conversion. In: Ricci CA (ed) The Antarctic region: geological evolution and processes. Terra Antartica Publication, Siena, pp 1087–1093

Danesi S, Morelli A (2001) Structure of the upper mantle under the Antarctic Plate from surface wave tomography. Geophys Res Letters 28:4395–4398

Della Vedova, et al. (1997) Crustal structure of the Transantarctic Mountains, western Ross Sea. In: Ricci CA (ed) The Antarctic region: geological evolution and processes. Terra Antartica Publication, Siena

Lawver L, Gahagan L (2003) Evolution of Cenozoic seaways in the Circum-Antarctic Region. Paleogrogr Paleoclimatol Paleoecol (in press)

Morelli A, Danesi S (2004) Seismological imaging of the Antarctic continental lithosphere: a review. Global Planet Change 42:155–165

Pondrelli S, Amato A, Chiappini M, Cimini GB, Colombo D, Di Bona M (1997) ACRUP1 Geotraverse: contribution of teleseismic sata recorded on land. In: Ricci CA (eds) The Antarctic region: geological evolution and processes. Terra Antartica Publication, Siena, pp 632–635

Ritzwoller MH, Shapiro NM, Leahy GM (2003) A resolved mantle anomaly as the cause of the Australian-Antarctic Discordance. J Geophys Re 108(7):2353

Rocchi S, Armienti P, D'Orazio M, Tonarini S, Wijbrans J, Di Vincenzo G (2002) Cenozoic magmatism in the western Ross embayment: role of mantle plume vs. plate dynamics in the development of the West Antarctic Rift System. J Geophys Res 107(9):2195

Silver PG (1996) Seismic anisotropy beneath the continents: probing the depth of geology. Ann Rev Earth Planet Sci 24:385–432

Silver PG, Chan WW (1988) Implication for continental structure and evolution from seismic anisotropy Nature 335:34–39

Silver PG, Chan WW (1991) Shear wave splitting and sub-continental mantle deformation. J Geophys Res 96:16429–16454

Savage MK (1999) Seismic anisotropy and mantle deformation: what have we learned from shear wave splitting? Rev Geophys 37:65–106

Salvini F, Storti F (1999) Cenozoic tectonic lineaments of the Terra Nova Bay region, Ross embayment, Antarctica. Global Planet Change 23:129–144

Salvini F, Brancolini G, Busetti M, Storti F, Mazzarini F, Coren F (1997) Cenozoic geodynamics of the Ross Sea region, Antarctica: crustal extension, intraplate strike-slip faulting, and tectonic inheritance. J Geophys Res 102(11):24669–24696

Vinnik LP, Farra V, Romanowicz B (1989) Azimuthal anisotropy in the Earth from observations of SKS at Geoscope and NARS broadband stations. Bull Seism Soc Amer 79:1542–1558

Wiens DA, Anandakrishnan S, Nyblade A, Fisher JL, Pozgay S, Shore PJ, Voigt D (2003) Preliminary results from the Trans-Antarctic Mountains Seismic Experiment (TAMSEIS). Terra Nostra 2003(4), Abstracts

Wilson TJ (1999) Cenozoic structural segmentation of the Transantarctic Mounatins rift flank in southern Victoria Land. Global Planet Change 23:105–127